frontiers | Frontiers in Materials

TYPE Original Research
PUBLISHED 07 June 2023
DOI 10.3389/fmats.2023.1193423

OPEN ACCESS

EDITED BY
Karin Larsson,
Uppsala University, Sweden

REVIEWED BY
P. J. Wei,
University of Science and Technology Beijing, China
Ziqi Yu,
Toyota Research Institute of North America, United States
Abdulkafi Mohammed Saeed,
Qassim University, Saudi Arabia

*CORRESPONDENCE
Nidhal Becheikh,
nidhal.becheikh@nbu.edu.sa
Khaled Lotfy,
khlotfy@zu.edu.eg

RECEIVED 24 March 2023
ACCEPTED 24 May 2023
PUBLISHED 07 June 2023

CITATION
El-Sapa S, El-Bary AA, Chtioui H, Becheikh N and Lotfy K (2023), Photothermal excitation in non-local semiconductor materials with variable moisture thermal conductivity according to moisture diffusivity.
Front. Mater. 10:1193423.
doi: 10.3389/fmats.2023.1193423

Photothermal excitation in non-local semiconductor materials with variable moisture thermal conductivity according to moisture diffusivity

Shreen El-Sapa[1], Alaa A. El-Bary[2,3,4], Houda Chtioui[5], Nidhal Becheikh[6]* and Khaled Lotfy[7,8]*

[1]Department of Mathematical Sciences, College of Science, Princess Nourah bint Abdulrahman University, Riyadh, Saudi Arabia, [2]Arab Academy for Science, Technology and Maritime Transport, Alexandria, Egypt, [3]National Committee for Mathematics, Academy of Scientific Research and Technology, Cairo, Egypt, [4]Council of Future Studies and Risk Management, Academy of Scientific Research and Technology, Cairo, Egypt, [5]Department of Physics, Faculty of Sciences, University of Monastir, Monastir, Tunisia, [6]College of Engineering, Northern Border University (NBU), Arar, Saudi Arabia, [7]Department of Mathematics, Faculty of Science, Zagazig University, Zagazig, Egypt, [8]Department of Mathematics, Faculty of Science, Taibah University, Madinah, Saudi Arabia

In this work, a new model is described for the case of interference between thermal, plasma and elastic waves in a non-local excited semiconductor medium. The governing equations have been put under the influence of moisture diffusion in one dimension (1D) when the moisture thermal conductivity of the non-local medium is taken in variable form. Linear transformations were used to describe the dimensionless model. The photo-thermoelasticity theory according to moisture diffusivity was applied to describe the governing equations using Laplace transforms to obtain analytical solutions. In the time domain, complete solutions are obtained linearly when the conditions are applied (thermal ramp type and non-Gaussian plasma shock) to the surface through numerical methods of inverse Laplace transforms. Numerical simulation is used to display the basic physical quantities under study graphically. The current research has yielded several specific examples of great significance. Many comparisons are made under the influence of fundamental physical variables such as relaxation times, variable thermal conductivity, non-local parameters, and reference moisture parameters through graphing and describing them theoretically.

KEYWORDS

photothermal theory, non-local semiconductor, moisture diffusivity, thermal conductivity, thermal ramp, silicon

1 Introduction

The combination of the "electronic deformation" in the semiconducting medium, based on the photogeneration theory in the crystal lattice, and the "thermoelastic mechanism" owing to the integral photothermal process characterizes an important thermoelastic fact. When atoms are perturbed, they migrate from a high-density to a low-density area. The mechanical defects and internal strains make this form of transportation conceivable. When temperatures climb to the point where materials begin to melt, atomic spacing increases. In a similar vein, moisture transfer takes place when an existing concentration gradient forms as a

result of the presence of unequal amounts of moisture. Temperature and humidity levels of the substance change depending on location and time. In this respect, the theories of heat transmission and moisture transfer are essentially identical. Mechanically applied stressors have the potential to significantly alter the distribution of temperature and moisture. That's why it is important to determine exactly how mechanical deformation relates to diffusion due to changes in humidity and temperature. Many practical engineering problems involve the interplay of moisture, heat, and deformation. When heat and moisture act on solids, a phenomenon known as hygrothermoelasticity takes place. Szekeres (2000); Szekeres (2012) examined how generalized heat transmission is affected by moisture. It has been suggested by Gasch et al. (2016) that changes in humidity and temperature could do more damage than mechanical loadings. Using a fundamental comparison between heat and moisture, (Szekeres and Engelbrecht, 2000) formulated equations governing coupled hygrothermoelasticity.

Photothermal (PT) analysis of semiconductor materials' thermal and electrical properties has grown in popularity. Semiconductors, used in sensors, solar cells, and advanced medical devices, have been extensively studied. Most renewable energy generation requires semiconductor knowledge. Semiconductors are dielectric and non-conductive. When optical energy activates semiconductor surface holes and electrons, electronic deformation occurs. The optical energy of light accelerates excited electrons to the surface, creating an electron cloud-like convective density or plasma waves. Photo-excitation and heat effect cause thermoelastic deformation. Thus, semiconductors are studied using thermoelasticity and photothermal theories. Numerous authors have developed novel methods to study photoacoustic spectroscopy's sensitivity when a laser beam hits a semiconductor sample (Gordon et al., 1964; Kreuzer, 1971). Photothermal approaches in several physical tests verified the nano-composite semiconductor materials' real temperatures, inner displacements, thermal diffusion, and other electrical properties (Tam, 1983; Tam, 1986; Tam, 1989; Todorovic et al., 1999; Song et al., 2010). Photo-excitation directly affects electronic deformation by causing elastic oscillations in the material's internal structures. Hobiny and Abbas (2016) studied photothermal waves in an unbounded medium using a semiconductor-filled cylindrical cavity. Two-temperature theory and strain-stresses in a semiconducting material under photothermal waves with hydrostatic starting stress are problematic (Abo-dahab and Lotfy, 2017; Lotfy, 2017). Lotfy (2016) applied the photo-thermoelasticity hypothesis to semiconductor media thermal-plasma-elastic waves under a magnetic field and rotation.

Alterations to a material's mechanical and thermal characteristics are often seen after a temperature change. The influence of the temperature gradient has been taken into consideration by several researchers after being ignored in previous studies of the expanded theory of thermoelasticity (Hasselman and Heller, 1980a; Youssef and Abbas, 2007a; Abouelregal and Marin, 2020; Marin et al., 2020). It is crucial to consider how temperature affects material characteristics (Marin et al., 2015) because the qualities of a material cannot be considered to have constant values under the effect of temperature change. The thermoelasticity theory emerged from discussions of coupled and uncoupled theories, both of which conflict with physical experiments. Biot (1956) introduced the unique hypothesis of linked thermoelasticity, which explained the anomaly. Infinite-speed thermal wave propagation was investigated using the CD theory. Lord and Shulman (1967) (LS) introduced a new concept when the heat equation was still in its infancy, by adding one relaxation period. Two relaxation periods were included in the heat conduction equation by Green and Lindsay (1972) (GL). The generalized thermoelasticity theory (GL) has been used by several writers (Chandrasekharaiah, 1986; Hosseini et al., 2013). Applications of the extended thermoelasticity theory including the interaction of thermal waves, electromagnetic fields, and mechanical waves in a thermoelastic solid medium are many.

Eringen (1972); Eringen and Edelen (1972) found that strain is defined as the gradient of the inner products of non-local deformations on non-local and local continuum components. This is a logical conclusion of the continuum theory of physics. Non-local thermoelastic theory (Eringen and Edelen, 1972) bridges the theoretical gap between the lattice-building theory and the classical continuum hypothesis. The classical continuum hypothesis allows for the investigation of constitutive relations between the atomic structure of lattices and the propagation of phonons. According to photomechanical waves and a moisture diffusivity process, (Alhashash et al., 2022) investigated the two-temperature thermoelasticity theory of a semiconductor model.

Physical characteristics of materials have been shown to depend on the temperature in recent studies. Deformation and thermo-mechanical behavior are both affected by the temperature dependency of these materials. The temperature-dependent thermal conductivity has a greater impact on thermal and mechanical behavior. Therefore, the thermal stress analysis is affected by the varying thermal conductivity. A thermoelastic hollow cylinder was an issue that Suhara investigated around the turn of the last century. Since then, several elastic and inelastic media issues have included the medium's temperature-dependent physical features (Hasselman and Heller, 1980b). Youssef (2005) used the state-space technique to the solution of the generalized thermoelasticity issue involving a spherical cavity where the thermal conductivity is temperature-dependent under ramp-type heating. Youssef and El-Bary (2006) have included variable thermal conductivity in the generalized thermoelasticity with thermal shock layers. Youssef and Abbas (2007b) have solved the generalized thermoelasticity issue for an infinitely long annular cylinder with variable thermal conductivity. Nano-energy uses rely heavily on the effects of size. For the first time, a new gradient theory is presented to characterize the nonlocal equation of motion (elastic nonlocality) in nano-scale materials during the coupled between electrons and thermoelastic fields (Allen, 2014; Khamis et al., 2021). On the other hand, the nanoscale systems are very complex, therefore, we contented ourselves with studying the non-local equation of motion only.

In this research, the moisture diffusivity property is used to study the wave propagation in a non-local semiconductor medium with photo-thermoelasticity. The work is investigated in one dimension (1D) while a photothermal transport process is going on, affected by specific mechanical forces and the diffusivity upon being hit by a non-Gaussian laser pulse. The problem has been addressed at the free surface of a non-local semiconducting material

when the thermal conductivity of the medium depends on the heat. By applying Laplace transforms to the time variable, the governing equations for the most important fundamental physical quantities may be solved analytically. Numerical inversion is carried out on a computer using powerful and efficient software. As a final step, normal force stress, normal displacement, carrier density, temperature distribution, and moisture concentration were all calculated numerically with the different values of thermal memory, thermal conductivity, moisture reference and nonlocality parameters.

2 The main equations

The carrier density $N(r_k,t)$ (optoelectronic), moisture concentration $m(r_k,t)$, temperature change $T(r_k,t)$, and displacement distribution $u(r_k,t)$ are all used to describe the novel model developed in this study (r_k is the position and t represents the time). The non-local medium's plasma-thermal-elastic wave equations interact with the moisture diffusion equations when the thermal conductivity is variable in the following tensor form (Sladek et al., 2020):

$$\frac{\partial N(r_i,t)}{\partial t} = D_E N_{,ii}(r_i,t) - \frac{N(r_i,t)}{\tau} + \frac{\kappa}{\tau}T(r_i,t) \tag{1}$$

$$\left.\begin{aligned} D_T\left(1+\tau_\theta\frac{\partial}{\partial t}\right)\left(K_m T_{,i}\right)_{,i} + D_T^m\left(K_m m_{,i}\right)_{,i} = \\ \left(1+\tau_q\frac{\partial}{\partial t}\right)\left(\rho C_e\frac{\partial \mathrm{T}(r_i,t)}{\partial t} + \gamma_t T_0\frac{\partial u_{i,j}(r_i,t)}{\partial t}\right) - \frac{E_g}{\tau}N(r_i,t) \end{aligned}\right\} \tag{2}$$

$$D_m\left(K_m m_{,i}\right)_{,i} + D_m^T\left(K_m T_{,i}\right)_{,i} = \frac{\partial}{\partial t}\left(K_m m(r_i,t)\right) - \frac{E_g}{\tau}N(r_i,t) + \gamma_m m_0 D_m\frac{\partial u_{j,j}(r_i,t)}{\partial t} \tag{3}$$

The non-local motion equation for diffusivity semiconductor medium may be written as:

$$\rho\left(1-\xi^2\nabla^2\right)\frac{\partial^2 u_i(r_i,t)}{\partial t^2} = \sigma'_{ij,j} \tag{4}$$

The nonlocal elastic parameter in length is denoted by ξ. The strain in terms of displacement takes the form:

$$\varepsilon_{ij} = \frac{1}{2}\left(u_{i,j} + u_{j,i}\right) \tag{5}$$

The stress equation in terms of plasma, temperature, strain and moisture concentration can be written as follows:

$$\left(1-\xi^2\nabla^2\right)\sigma_{ij} = \sigma'_{ij} = C_{ijkl}\varepsilon_{kl} - \beta_{ij}\left(\alpha_t\left(1+\tau_\theta\frac{\partial}{\partial t}\right)T + d_n N\right) - \beta_{ij}^m m, \quad i,j,k,l = 1,2,3 \tag{6}$$

In all equations in this work a "comma" before an index implies space-differentiation and a "dot" above a symbol refers to the time-differentiation.

Take into account the moisture thermal conductivity, which is variable and may be chosen as a linear function of temperature. Non-local semiconductor material's changing moisture thermal conductivity under the effect of a light heat source is represented as a function of temperature as shown in (Hasselman and Heller, 1980b; Alhashash et al., 2022):

$$K_m = K_0(1+\pi T) \tag{7}$$

When the medium is independent of temperature, the constant thermal conductivity (reference) is K_0 and π represents a negative small parameter. The integral form of thermal conductivity may be derived using the Kirchhoff transform to convert the nonlinear temperature components into linear ones (Hasselman and Heller, 1980b; Alhashash et al., 2022):

$$\vartheta = \frac{1}{K_0}\int_0^T K_m(z)dz \tag{8}$$

Considering that the values of all physical quantities are unrelated to the yz-coordinates, all studies are performed along the x-axis (the direction of wave propagation is along the x-axis). The main Eqs. 1, 4 involving the physical variables may be recast in 1D as follows (Hasselman and Heller, 1980a):

$$\frac{\partial N}{\partial t} = D_E\frac{\partial^2 N}{\partial x^2} - \frac{N}{\tau} + \frac{\kappa}{\tau}T \tag{9}$$

The motion Eq. 4 has the following structure (Hasselman and Heller, 1980b):

$$\rho\left(1-\xi^2\frac{\partial^2}{\partial x^2}\right)\frac{\partial^2 u}{\partial t^2} = (2\mu+\lambda)\frac{\partial^2 u}{\partial x^2} - \gamma_t\left(1+\tau_\theta\frac{\partial}{\partial t}\right)\frac{\partial T}{\partial x} - \delta_n\frac{\partial N}{\partial x} - \gamma_m\frac{\partial m}{\partial x} \tag{10}$$

Where $\gamma_{t,m} = \beta\,\alpha_{m,T}$ and $\delta_n = \beta d_n, \beta = 3\mu + 2\lambda$.

Several methods of differentiation provide Eqs. 7, 8 for the map transform, which may be used to the fundamental equations to derive the thermal conductivity, which is a variable in the original computations, as:

$$\left.\begin{aligned} K_0\vartheta_{,i} = K_m T_{,i}, \\ K_0\vartheta_{,ii} = \left(K_m T_{,i}\right)_{,i}, \\ \left(K_0/K_m\right)\vartheta_{,i} = T_{,i}. \end{aligned}\right\} \tag{11}$$

Using the same technique, the time-differentiating from the first order for diffusivity is:

$$K_0\frac{\partial \mathrm{M}}{\partial t} = K_m\frac{\partial m}{\partial t} \tag{12}$$

As a result applying the map transform to Eq. 1, which $\frac{\partial}{\partial x_i}$ may act on both sides, yields:

$$\left.\begin{aligned} \frac{\partial}{\partial t}\frac{\partial N}{\partial x_j} = D_E\frac{\partial N_{,ii}}{\partial x_j} - \frac{1}{\tau}\frac{\partial N}{\partial x_j} + \frac{\kappa}{\tau}\frac{\partial T}{\partial x_j}, \\ \frac{\partial}{\partial t}\frac{\partial N}{\partial x_j} = D_E\frac{\partial N_{,ii}}{\partial x_j} - \frac{1}{\tau}\frac{\partial N}{\partial x_j} + \frac{\kappa K_0}{\tau K_m}\frac{\partial \vartheta}{\partial x_j}, \\ \frac{\partial}{\partial t}\frac{\partial N}{\partial x_j} = D_E\frac{\partial N_{,ii}}{\partial x_j} - \frac{1}{\tau}\frac{\partial N}{\partial x_j} + \frac{\kappa}{\tau}\frac{\partial \vartheta}{\partial x_j}. \end{aligned}\right\} \tag{13}$$

The last term in the first half of Eq. 13 in the preceding equation may be extended as follows if the non-linear components are disregarded:

$$\left.\begin{aligned}\frac{\kappa K_0}{\tau K_m}\frac{\partial \vartheta}{\partial x}=\frac{\kappa K_0}{K_0(1+\pi T)}\frac{\partial \vartheta}{\partial x}=\kappa(1+\pi T)^{-1}\frac{\partial \vartheta}{\partial x}=\frac{\kappa}{\tau}(1-\pi T+(\pi T)^2-.....)\frac{\partial \vartheta}{\partial x}=\\ \frac{\kappa}{\tau}\frac{\partial \vartheta}{\partial x}-\frac{\kappa}{\tau}\pi T\frac{\partial \vartheta}{\partial x}+\frac{\kappa}{\tau}(\pi T)^2\frac{\partial \vartheta}{\partial x}-.....=\frac{\kappa}{\tau}\frac{\partial \vartheta}{\partial x}\end{aligned}\right\} \tag{14}$$

Leibniz integral rule is applied to Eq. 13, which yields:

$$\frac{\partial N}{\partial t}=D_E N_{,ii}-\frac{1}{\tau}N+\frac{\kappa}{\tau}\vartheta. \tag{15}$$

Rewriting the heat Eq. 2 and moisture diffusion Eq. 3 after using the map transform yields the following:

$$D_T\left(1+\tau_\theta\frac{\partial}{\partial t}\right)\vartheta_{,ii}+D_T^m M_{,ii}=\left(1+\tau_q\frac{\partial}{\partial t}\right)\left(\frac{1}{k}\frac{\partial \vartheta}{\partial t}+\frac{\gamma_t T_0}{K_0}\frac{\partial u_{i,j}}{\partial t}\right)-\frac{E_g}{K_0\tau}N \tag{16}$$

$$D_m M_{,ii}+D_m^T\vartheta_{,ii}=\frac{\partial M}{\partial t}-\frac{E_g}{K_0\tau}N+\frac{\gamma_m m_0 D_m}{K_0}\frac{\partial u_{i,j}}{\partial t} \tag{17}$$

According to the map transform, the equation of motion (4) takes the form:

$$\rho\left(1-\xi^2\frac{\partial^2}{\partial x^2}\right)\frac{\partial^2 u}{\partial t^2}=(2\mu+\lambda)\frac{\partial^2 u}{\partial x^2}-\gamma_t\left(1+\tau_\theta\frac{\partial}{\partial t}\right)\frac{K_0}{K_m}\frac{\partial \vartheta}{\partial x}-\delta_n\frac{\partial N}{\partial x}-\gamma_m\frac{K_0}{K_m}\frac{\partial M}{\partial x} \tag{18}$$

With neglecting the non-linear term, yields:

$$\frac{K_0}{K_m}\frac{\partial \vartheta}{\partial x}=\frac{K_0}{K_0(1+\pi T)}\frac{\partial \vartheta}{\partial x}=(1+\pi T)^{-1}\frac{\partial \vartheta}{\partial x}=(1-\pi T+(\pi T)^2-.....)\frac{\partial \vartheta}{\partial x}=\frac{\partial \vartheta}{\partial x} \tag{19}$$

According to relation (19), the mapped motion Eq. 18 can be rewritten as:

$$\rho\left(1-\xi^2\frac{\partial^2}{\partial x^2}\right)\frac{\partial^2 u}{\partial t^2}=(2\mu+\lambda)\frac{\partial^2 u}{\partial x^2}-\gamma_t\left(1+\tau_\theta\frac{\partial}{\partial t}\right)\frac{\partial \vartheta}{\partial x}-\delta_n\frac{\partial N}{\partial x}-\gamma_m\frac{\partial M}{\partial x} \tag{20}$$

On the other hand, the constitutive equation for the non-local medium can be rewritten in 1D as:

$$\left(1-\xi^2\frac{\partial^2}{\partial x^2}\right)\sigma_{xx}=(2\mu+\lambda)\frac{\partial u}{\partial x}-\beta(\alpha_t\vartheta+d_n N)-\gamma_m M=\sigma \tag{21}$$

3 Mathematical formulation

The following are additional non-dimensional values we may provide for use in simplifying expressions:

$$(x',\xi',u')=\frac{(x,\xi,u)}{C_T t^\star},\left(t',\tau_q',\tau_\theta'\right)=\frac{\left(t,\tau_q,\tau_\theta\right)}{t^\star},(\vartheta',N')=\frac{(\gamma_t\vartheta,\delta_n N)}{2\mu+\lambda},\sigma'=\frac{\sigma}{\mu},M'=M \tag{22}$$

Using the dimensionless Eq. 22, the mapped Eqs. 15–17 and Eqs. 20, 21 can be reduced in the following form:

$$\left(\frac{\partial^2}{\partial x^2}-q_1-q_2\frac{\partial}{\partial t}\right)N+\varepsilon_3\,\vartheta=0 \tag{23}$$

$$\left(\left(1+\tau_\theta\frac{\partial}{\partial t}\right)\frac{\partial^2}{\partial x^2}-a_1\left(1+\tau_q\frac{\partial}{\partial t}\right)\frac{\partial}{\partial t}\right)\vartheta+a_2\frac{\partial^2 M}{\partial x^2}+a_3 N-\varepsilon_1\left(1+\tau_q\frac{\partial}{\partial t}\right)\frac{\partial^2 u}{\partial t\partial x}=0 \tag{24}$$

$$\left(\frac{\partial^2}{\partial x^2}-a_4\frac{\partial}{\partial t}\right)M+a_5\frac{\partial^2 \vartheta}{\partial x^2}+a_6 N-a_7\frac{\partial^2 u}{\partial t\partial x}=0 \tag{25}$$

$$\left(\frac{\partial^2}{\partial x^2}-\left(1-\xi^2\frac{\partial^2}{\partial x^2}\right)\frac{\partial^2}{\partial t^2}\right)u-\left(1+\tau_\theta\frac{\partial}{\partial t}\right)\frac{\partial \vartheta}{\partial x}-\frac{\partial N}{\partial x}-a_8\frac{\partial M}{\partial x}=0 \tag{26}$$

$$\sigma=a_9\left(\frac{\partial u}{\partial x}-(\vartheta+N)\right)-a_{10}M \tag{27}$$

Where

$$q_1=\frac{kt^\star}{D_E\rho\tau C_e},\quad q_2=\frac{k}{D_E\rho C_e},\quad a_1=\frac{C_T^2 t^\star}{kD_T},\quad a_2=\frac{D_T^m\gamma_t}{D_T(2\mu+\lambda)},$$
$$\varepsilon_2=\frac{\alpha_T E_g t^\star}{\tau d_n\rho C_e},\quad a_3=\varepsilon_2 a_1\varepsilon_1=\frac{\gamma_t^2 T_0 t^\star}{K_0\rho},\quad a_4=\frac{C_T^2 t^\star}{D_m},$$
$$a_5=\frac{D_m^T(2\mu+\lambda)}{D_m\gamma_t},\quad a_6=\frac{E_g(2\mu+\lambda)t^\star a_4}{K_0\delta_n\tau},\quad a_7=\frac{\gamma_m m_0 C_T^2 t^\star}{K_0},$$
$$a_8=\frac{\gamma_m}{2\mu+\lambda}\varepsilon_3=\frac{d_n K_0\kappa t^\star}{\alpha_T\rho\tau C_e D_E},\quad a_9=\frac{2\mu+\lambda}{\mu},$$
$$a_{10}=\frac{\gamma_m}{\mu}C_T^2=\frac{2\mu+\lambda}{\rho},\quad \delta_n=(2\mu+3\lambda)d_n,\quad D_T=\frac{k}{\rho C_e},$$
$$t^\star=\frac{k}{\rho C_e C_T^2}$$

To aid in finding a mathematical solution when the system is initially at rest, below are the initial conditions:

$$u(x,t)|_{t=0}=\left.\frac{\partial u(x,t)}{\partial t}\right|_{t=0}=0,\quad T(x,t)|_{t=0}=\left.\frac{\partial T(x,t)|}{\partial t}\right|_{t=0}=0,$$
$$m(x,t)|_{t=0}=\left.\frac{\partial m(x,t)}{\partial t}\right|_{t=0}=0$$
$$\sigma(x,t)|_{t=0}=\left.\frac{\partial \sigma(x,t)}{\partial t}\right|_{t=0}=0,$$
$$N(x,t)|_{t=0}=\left.\frac{\partial N(x,t)}{\partial t}\right|_{t=0}=0 \tag{28}$$

4 The solution to the problem

To simplify the definition of partial differential equations, the Laplace transform is used, which is defined as:

$$L(\mathrm{X}(x,t))=\bar{\mathrm{X}}(x,s)=\int_0^\infty \exp(-st)\mathrm{X}(x,t)\,dt \tag{29}$$

Eq. 29 is used to convert Eqs. 23–27 as follows:

$$(D^2-\alpha_1)\bar{N}+\varepsilon_3\,\bar{\vartheta}=0 \tag{30}$$

$$\left(D^2-\alpha_2\right)\bar{\vartheta}+a_2^{'}D^2\,\bar{M}+a_3^{'}\,\bar{N}-\alpha_3\,D\bar{u}=0 \tag{31}$$

$$\left(D^2-\alpha_4\right)\bar{M}+a_5D^2\bar{\vartheta}+a_6\,\bar{N}-\alpha_5\,D\bar{u}=0 \tag{32}$$

$$\left(D^2-\mathbb{Q}\right)\bar{u}-\mathbb{Z}D\left(\wp\bar{\vartheta}+N-\mathbb{R}D\bar{M}\right)=0 \tag{33}$$

$$\bar{\sigma}=a_9\left(D\bar{u}-\left(\bar{\vartheta}+\bar{N}\right)\right)-a_{10}\bar{M} \tag{34}$$

where, $D=\frac{d}{dx}$, $\mathbb{R}=\frac{a_8}{1+\xi^2s^2}$, $\mathbb{Z}=\frac{1}{1+\xi^2s^2}$, $\alpha_1=q_1+q_2s$, $\mathbb{Q}=\frac{s^2}{(1+\xi^2s^2)}$, $\alpha_2=\frac{a_1\,(1+\tau_qs)s}{(1+\tau_\theta s)}$, $a_2^{'}=\frac{a_2}{(1+\tau_\theta s)}$, $\alpha_4=a_4s$, $\wp=1+\tau_\theta s$, $\alpha_5=a_7s$, $\alpha_3=\varepsilon_1\frac{(1+\tau_qs)s}{(1+\tau_\theta s)}a_3=\frac{a_3}{(1+\tau_\theta s)}$.

Eliminating technique is used for the quantities $\bar{\vartheta},\bar{u},\bar{N}$ and $\bar{M}$ using Mathematica softwear; yields

$$\left(D^8-\Theta_1D^6+\Theta_2D^4-\Theta_3D^2-\Theta_4\right)\{\bar{M},\bar{N},\bar{\vartheta},\bar{u}\}(x,s)=0 \tag{35}$$

By conducting calculations using computer programs such as Mathematica, the basic coefficients can be calculated in Eq. 35, whose values are deduced as follows:

$$\left.\begin{aligned}
\Theta_1&=-\frac{\left\{-\mathbb{Q}a_2a_5-a_2^{'}a_5\alpha_1-a_5\mathbb{R}\alpha_3+\mathbb{Q}-a_2\alpha_5+\mathbb{R}\alpha_5+\mathbb{Z}\wp\alpha_1+\alpha_2+\alpha_3+\alpha_4\right\}}{\left(a_3^{'}a_2^{'}-1\right)},\\
\Theta_2&=\frac{\left\{\begin{array}{c}\mathbb{Q}a_2^{'}a_5\alpha_1+a_5\mathbb{R}\alpha_1\alpha_3-\mathbb{Q}\left(\alpha_1+\alpha_2+\alpha_4\right)-a_2^{'}a_7\varepsilon_3+a_2^{'}\alpha_1\alpha_5+\\ a_2\alpha_5\varepsilon_3-\mathbb{R}\left(\alpha_1\alpha_5+\alpha_2\alpha_5\right)+\mathbb{Z}a_3\varepsilon_3-\alpha_1\alpha_2-\alpha_1\alpha_3-\mathbb{Z}\wp\alpha_1\alpha_4-\\ \alpha_2\alpha_4-\alpha_3\alpha_4-\alpha_3\varepsilon_3\end{array}\right\}}{\left(a_3^{'}a_2^{'}-1\right)},\\
\Theta_3&=-\frac{\left\{\begin{array}{c}\mathbb{Q}\left(a_2^{'}a_7\varepsilon_3-a_3^{'}\varepsilon_3+\mathbb{Z}\alpha_1\alpha_2+\alpha_1\alpha_4+\alpha_2\alpha_4\right)-a_3^{'}\mathbb{R}\alpha_5\varepsilon_3\\ +a_7\mathbb{R}\alpha_3\varepsilon_3+\mathbb{R}\alpha_1\alpha_2\alpha_5-a_3^{'}\alpha_4\varepsilon_3+\alpha_1\alpha_2\alpha_4+\mathbb{Z}\wp\alpha_1\alpha_3\alpha_4+\alpha_3\alpha_4\varepsilon_3\end{array}\right\}}{\left(a_3^{'}a_2^{'}-1\right)},\\
\Theta_4&=\mathbb{Q}\frac{\left\{a_3^{'}\alpha_4\varepsilon_3-\mathbb{Z}\wp\alpha_1\alpha_2\alpha_4\right\}}{\left(a_3^{'}a_2^{'}-1\right)}.
\end{aligned}\right\} \tag{36}$$

Eq. 35 can be solved using the factorization method, which yields:

$$\left(D^2-m_1^2\right)\left(D^2-m_2^2\right)\left(D^2-m_3^2\right)\left(D^2-m_4^2\right)\{\bar{\vartheta},\bar{u},\bar{N},\bar{M}\}(x,s)=0 \tag{37}$$

To acquire roots in the positive real part at $x\to\infty$, substitute $m_i^2\,(i=1,2,3,4)$. Since this is a linear problem, the solution to Eq. 37 takes the form below.

$$\bar{\vartheta}(x,s)=\sum_{i=1}^{4}D_i(s)\,e^{-m_ix} \tag{38}$$

It is possible to express the solutions in terms of the other variables as follows:

$$\bar{N}(x,s)=\sum_{i=1}^{4}D_i^{'}(s)\,e^{-m_ix}=\sum_{i=1}^{4}H_{1i}D_i(s)\,e^{-m_ix} \tag{39}$$

$$\bar{u}(x,s)=\sum_{i=1}^{4}D_i^{''}(s)\exp\left(-m_ix\right)=\sum_{i=1}^{4}H_{2i}\,D_i(s)\exp\left(-m_ix\right) \tag{40}$$

$$\bar{M}(x,s)=\sum_{i=1}^{4}D_i^{'''}(s)\exp\left(-m_ix\right)=\sum_{i=1}^{4}H_{3i}\,D_i(s)\exp\left(-m_ix\right) \tag{41}$$

$$\bar{\sigma}\,(x,s)=\sum_{i=1}^{4}D_i^{(4)}(s)\exp\left(-m_ix\right)=\sum_{i=1}^{4}H_{4i}\,D_i(s)\exp\left(-m_ix\right) \tag{42}$$

The quantities $D_i,D_i^{'},D_i^{''}$, and $D_i^{'''}\;(i=1..4)$ are the unknown parameters. The following relationship exists between the unknown parameters and may be determined using the basic Eqs 30–34:

$$H_{1i}=\frac{-\varepsilon_3}{m_i^{\,2}-\alpha_1},$$

$$H_{2i}=\frac{(a_2-\mathbb{R})m_i^4+\left(-a_2^{'}\alpha_1-\mathbb{Z}a_2^{'}\varepsilon_3+\mathbb{R}\left(\alpha_1+\alpha_2\right)\right)m_i^2+\mathbb{R}\left(a_3^{'}\varepsilon_3-\alpha_1\alpha_2\right)}{m_i\left(m_i^4a_2^{'}+\left(-\mathbb{Q}a_2^{'}-\mathbb{Z}a_2^{'}\alpha_1-\mathbb{R}\alpha_3\right)m_i^2+\mathbb{Q}a_2^{'}\alpha_1+\mathbb{R}\alpha_1\alpha_3\right.},$$

$$H_{3i}=-\frac{\left(\begin{array}{c}\left(m_i^6+\left(-\mathbb{Q}-\mathbb{Z}\alpha_1-\alpha_2-\alpha_3\right)m_i^4+\left(\mathbb{Q}\left(\alpha_1+\alpha_2\right)-\right.\right.\\ \left.\left.a_3^{'}\varepsilon_3+\mathbb{Z}\alpha_1\alpha_2+\alpha_3\left(\alpha_1+\varepsilon_3\right)\right)m_i^2+\mathbb{Q}\left(a_3^{'}\varepsilon_3-\alpha_1\alpha_2\right)\end{array}\right)}{\left(\left(m_i^2-\alpha_1\right)\left(m_i^2a_2^{'}-\mathbb{Q}a_2^{'}-\mathbb{R}\alpha_3\right)m_i^2\right)},$$

$$H_{4i}=a_9\left(m_iH_{2i}-\left(1+H_{1i}\right)\right)-a_{10}H_{3i}$$

5 Boundary conditions

Assume that the elastic non-local semiconductor medium is exposed to thermal loads of the thermal ramp type under conditions of heat, plasma, and mechanical loading. These conditions are applied to the free outside surface of the non-local medium. In every scenario, Laplace transformations are used (Vlase et al., 2017; Sladek et al., 2020).

(I) Type ramp heating is used for the thermal boundary condition at $x=0$, which may be expressed according to the thermal excitation function $F(t)$:

$$\vartheta(0,t)=\begin{cases}0 & t\le 0\\ \dfrac{t}{t_0} & 0<t\le t_0\\ 1 & t>t_0\end{cases} \tag{43}$$

The time of pulse heat flux is $t_0=0.001$, Equation 43 is solved by the use of Laplace transforms and the attribute of being dimensionless, whereby:

$$\sum_{n=1}^{4}D_i(s)=\bar{F}(s)\frac{(1-e^{-st_0})}{t_0s^2} \tag{44}$$

(II) A mechanical load is applied to the surface at $x=0$. This means that for a generalized non-local photo-thermoelastic medium with an orthotropic boundary, the boundary conditions are provided according to a given hydrostatic initial stress function $q(t)$ by:

$$\sigma(x,t)=q(t) \tag{45}$$

Laplace transformation is used, which yields:

$$\sum_{i=1}^{4}\{a_9\left(m_iH_{2i}-\left(1+H_{1i}\right)\right)-a_{10}H_{3i}\}\left(D_i\right)=\bar{q}(s) \tag{46}$$

(III) During the diffusion phase, the carriers' plasma density, which can be quantified with the help of the plasma excitation function $N^{\star}$, may reach the sample's surface at $x=0$ due to the low chance of recombination. In this case, it is assumed that a laser excitation is supplied to a non-local semiconductor surface in the form of a non-Gaussian plasma shock loading as:

$$N(x,s)=N^{\star}=N_0^{*}t\exp\left(-\frac{t}{t_p}\right) \tag{47}$$

Maximum plasma shock loading caused by a laser pulse occurs at a time $t_p=t$, denoted by N_0^{*}. According to Laplace transform, yields:

TABLE 1 physical constants of Si material.

Name (unit)	Symbol	Value
Lamé's constants (N/m^2)	$\lambda\ \mu$	6.4×10^{10}, 6.5×10^{10}
Density (kg/m^3)	ρ	2330
Absolute temperature (K)	T_0	800
The photogenerated Carrier lifetime (s)	τ	$5\text{x}\,10^{-5}$
The carrier diffusion coefficient (m^2/s)	D_E	2.5×10^{-3}
the coefficient of electronic deformation (m^3)	d_n	$-9\,\text{x}\,10^{-31}$
The energy gap (eV)	E_g	1.11
The coefficient of linear thermal expansion (K^{-1})	α_t	$4.14\text{x}\,10^{-6}$
The thermal conductivity of the sample $(Wm^{-1}K^{-1})$	k	150
Specific heat at constant strain $(J/(kg\,K))$	C_e	695
The recombination velocities (m/s)	s	2
Temperature diffusivity	D_T	$\frac{k}{\rho C_e}$
The coupled diffusivities $(m^2(\%H_2O)/s(K)),$ $(m^2 s(K)/(\%H_2O))$	D_T^m	2.1×10^{-7}
	D_m^T	0.648×10^{-6}
References moisture	m_0	10%
The diffusion constants of moisture $(m^2 s^{-1})$	D_m	0.35×10^{-2}
The moisture thermodiffusion constant $(cm/cm(\%H_2o))$	α_m	2.68×10^{-3}
The moisture diffusivity (kg/msM)	k_m	2.2×10^{-8}

$$\bar{N}(0,s) = \sum_{i=1}^{4} H_{1i} D_i(0,s) = \frac{N_0^{\star}}{\left(s + 1/t_p\right)^2} \tag{48}$$

(IV) The boundary condition for displacement on the free surface at $x = 0$ is:

$$\bar{u}(0,s) = 0 \tag{49}$$

Or:

$$\sum_{i=1}^{4} H_{2i} D_i(x,s) = 0 \tag{50}$$

To obtain the relation between the temperature T and the mapped temperature ϑ, using the map and integral Eqs. 7, 8, yields:

$$\vartheta = \frac{1}{K_0}\int_0^T K_0(1 + \pi T)dT = T + \frac{\pi}{2}T^2 = \frac{\pi}{2}\left(T + \frac{1}{\pi}\right)^2 - \frac{1}{2\pi} \tag{51}$$

$$T = \frac{1}{\pi}\left[\sqrt{1 + 2\pi\vartheta} - 1\right] \tag{52}$$

In the same way, moisture diffusivity can be obtained.

6 Inversion of the laplace transforms

The inverse Laplace-transform is calculated using the Riemann-sum approximation method; [see ref. (Honig and Hirdes, 1984)] for additional information. Therefore, the following expressions may be used to derive the field's time-domain variables based on Fourier series expansion. For a Laplace-domain function $\bar{\zeta}(x,s)$, the transfer to the time domain looks like this:

$$\zeta(x,t') = L^{-1}\left\{\bar{\zeta}(x,s)\right\} = \frac{1}{2\pi i}\int_{n-i\,\infty}^{n+i\infty} \exp(st')\bar{\zeta}(x,s)ds \tag{53}$$

where $s = n + i\mathrm{M}$ $(n, \mathrm{M} \in R)$. Consequently, the equation with its variables changed around may be expressed as:

$$\zeta(x,t') = \frac{\exp(nt')}{2\pi}\int_{-\infty}^{\infty} \exp(i\beta t)\bar{\zeta}(x, n + i\beta)d\beta \tag{54}$$

The following relationship may be found by expanding for the function $\zeta(x,t')$ in the closed interval $[0, 2t']$ using the Fourier series:

$$\zeta(x,t') = \frac{e^{nt'}}{t'}\left[\frac{1}{2}\bar{\zeta}(x,n) + Re\sum_{k=1}^{\mathfrak{R}}\bar{\zeta}\left(x, n + \frac{ik\pi}{t'}\right)(-1)^n\right] \tag{55}$$

Where i and Re indicate the imaginary number unit and the real component, respectively, adequate $\mathfrak{R}$ stands for the number of terms in the equation. The value of the parameter n may be determined based on the instructions in (Honig and Hirdes, 1984). Because of this, a method known as numerical inversion of the Laplace transform (NILT) is used (Brancik, 1999). This approach is based on the quick Fourier transform.

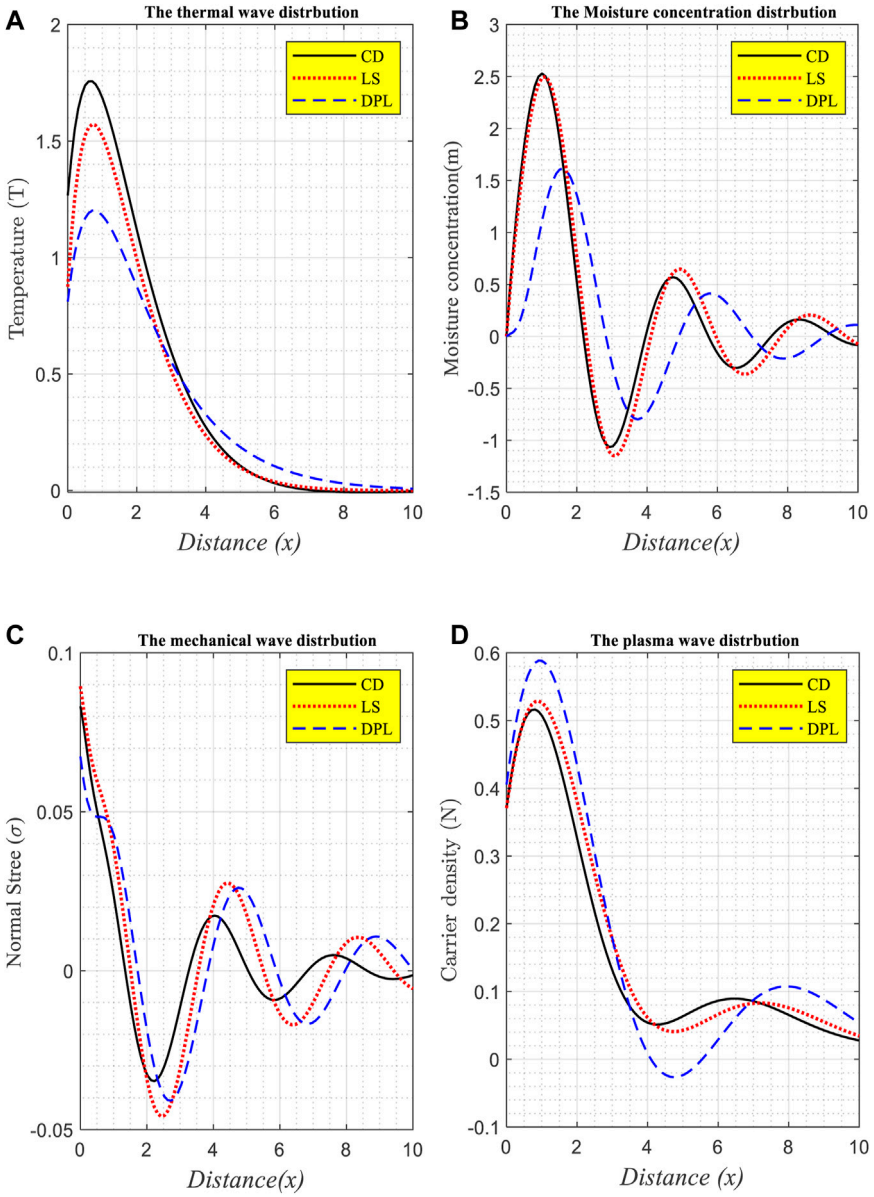

FIGURE 1
(A–D) The wave propagation of the physical fields distribution against the distance according to the variation of thermal relaxation times under the effect of variable thermal conductivity and moisture field for non-local Si material.

7 Numerical results and discussions

To further demonstrate the theoretical findings from the preceding part, we will now provide numerical data. Numerical values of physical characteristics such as thermal, displacement, plasma, moisture concentration, and the normal distribution of stress obtained from this problem under the impact of variable thermal conductivity over a short time may now be graphically represented in MATLAB for the researched physical fields. In the theoretical investigation, n-type silicon (Si) acts as the non-local semiconductor solid material in the device. Table 1 uses SI units for the following Si physical parameters: (Lotfy et al., 2017; Ezzat, 2020; Mondal and Sur, 2021; Zhao et al., 2022a; Zhao et al., 2022b).

7.1 The impact of thermal relaxation times

Three thermoelasticity models with various relaxation times are analyzed in Figure 1A–D (the first group). When $\tau_\theta = \tau_q = 0$, the first model illustrates coupled thermoelasticity (CT) theory. It would seem that the Lord and Shulman (LS) model enters the central equations at $\tau_\theta = 0$. Lastly, when we put $0 \leq \tau_\theta = 0.0002 < \tau_q = 0.0003 = 0$, we see the dual phase lag (DPL) model. The principal physical fields are shown against the horizontal distance in the range $0 \leq x \leq 10$ in this figure, with the effect of moisture diffusivity at a reference moisture of $m_0 = 30\%$, variable thermal conductivity when $\pi = -0.06$ and laser pulses for Si material at a non-local parameter value of $\xi = 0.5$ (Scutaru et al.,

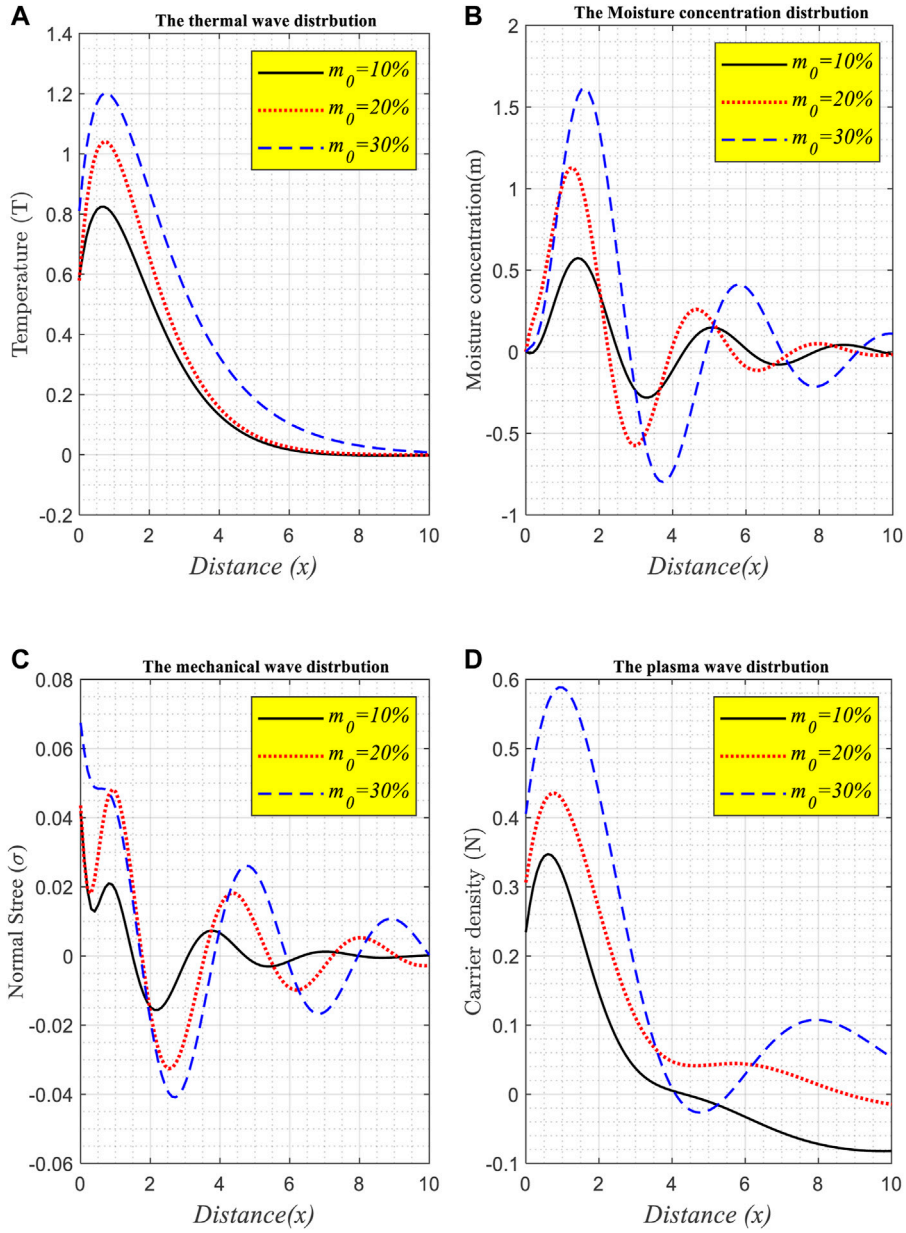

FIGURE 2
(A–D) The wave propagation of the physical fields distribution against the distance according to the different values the reference moisture m_0 under the influence of the DPL model and variable thermal conductivity for the non-local Si material.

2020). Because of photo-excitation according to the ramp type heating, laser shock, and moisture diffusivity, both the temperature (thermal wave) and carrier density (plasma wave) distributions begin with positive values near the surface and steadily grow in the first range, reaching their highest values close to the surface. This is because, when subjected to laser pulses, they meet the necessary temperature and recombination conditions. At greater distances from the surface, however, both distributions (thermal and plasma waves) gradually decrease with exponential behavior to approach the minimum value. Each distribution eventually converges on the zero line, attaining a steady state, as the distance between them grows with increasing depth into the semiconductor material. The temperature and plasma distributions shown here are in agreement with the experimental data from Liu et al. (2022). Distance-dependent moisture concentration (moisture wave m) is seen in the second subfigure. The surface requirement is met and the distribution of moisture concentration starts at zero in all three model circumstances. However, due to the influence of laser pulses and thermal shock ramp type on the surface, the distribution of moisture exhibits wavelike behavior, beginning with a very gradual rise near the surface and reaching a maximum value before beginning to fall until reaching an absolute minimum value. As the distribution moves deeper from the surface, it

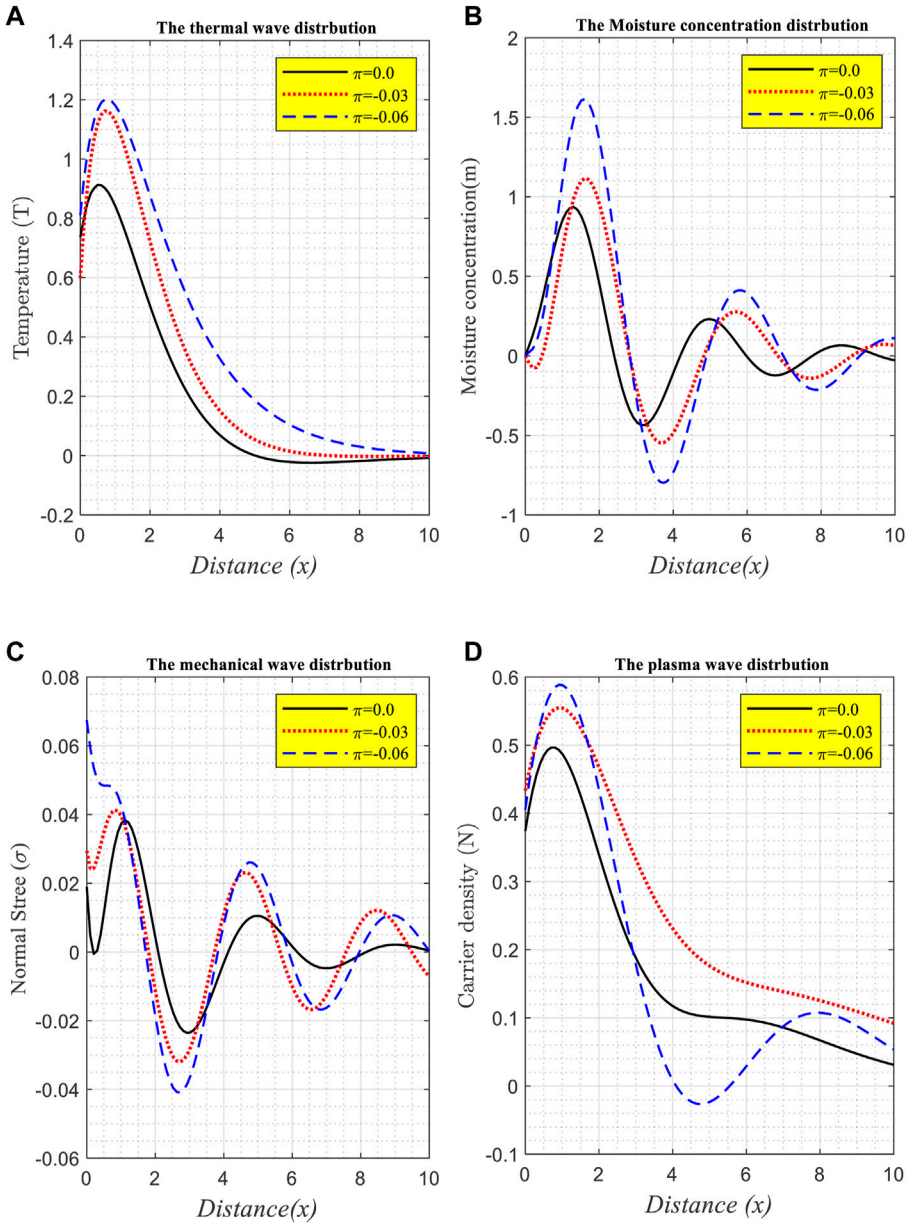

FIGURE 3
(A–D) The wave propagation of the physical fields distribution against the distance according to the variation of thermal conductivity under the effect of moisture field for non-local Si material using the DPL model.

alternates between periods of growth and decay until the wave dies out deep inside the non-local semiconducting material and equilibrium is reached. The third subfigure demonstrates, following different thermoelastic models, how the mechanical load creates the amplitude of the mechanical force σ (stress distribution) with an increase in the value of the distance. By applying a mechanical load to the surface, the mechanical distribution begins with a maximum positive value, as shown in this subfigure, and then declines progressively until it approaches the absolute minimum value. In response to the nonlocality effect, the wave propagation initially increases as one moves away from the surface, reaching a maximum value before gradually decreasing and increasing cyclically, taking on a wave behavior, and eventually disappearing altogether as one furthers from the surface to achieve mechanical equilibrium (Alhashash et al., 2022).

7.2 Impact of reference moisture

Figure 2A–D (the second category) presents a representation of the physical quantities plotted against a horizontal distance and accompanied by several reference moisture constant values. Under the impact of laser pulses and variable thermal

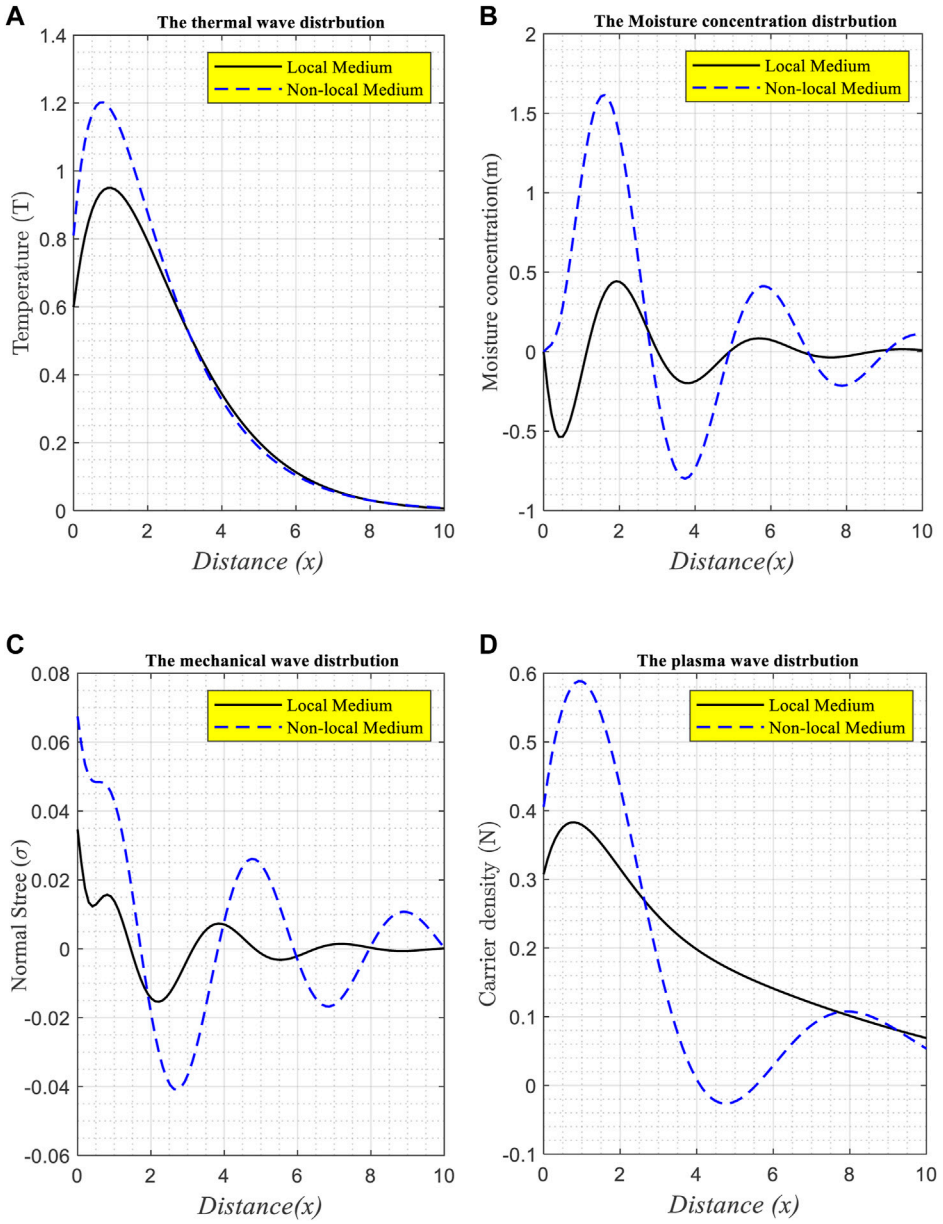

FIGURE 4
(A–D) The wave propagation of the physical field distribution against the distance according to the local and non-local parameters under the effect of variable thermal conductivity and moisture field for Si material.

conductivity $\pi = -0.06$, all computations are carried out using the DPL model for non-local silicon (Si) material. Figure 2 (the second category) illustrates the variation of the physical fields associated with the distance about three different scenarios of reference moisture m_0: (= 10% , = 20% and = 30%). This graphic makes it clear how the behavior of wave propagation varies depending on factors such as the concentration of moisture, the stress force, the temperature distributions, and the carrier density distribution. The wave distribution of the major quantities follows essentially the same behavior as shown in Figure 1, as seen in this figure; however, the distribution varies depending on the value of the reference moisture. This is something that we notice after looking at this figure.

7.3 The effect of the variable thermal conductivity

According to the kind of thermal ramp and the three constant values of π, Figure 3A–D depicts the changes in the thermal, moisture, stress, and plasma distributions with distance for dimensionless time constants ($t = 0.004$) and moisture reference m_0=30%. These three numbers $\pi = 0$, $\pi = -0.03$ and $\pi = -0.06$, are constants. On the non-local model, we are now attempting to explain physical domain variables. According to DPL theory, the principal physical fields of the constant value of $\pi = 0$ being investigated, but the other two values $\pi = -0.03$ and $\pi = -0.06$ are entirely differently described (when the non-local

medium is temperature dependent). Under the impact of various values of the variable thermal conductivity, the fluctuation of the physical field variables varies. We may therefore conclude that changes in the variable thermal conductivity, particularly when it is heat dependent, have an impact on the characteristics of all physical field variables (Lotfy and Tantawi, 2020; Huang et al., 2021).

7.4 The comparison according to the nonlocallty paramter

At a constant value of time ($t = 0.004$), $\pi = -0.06$, $m_0 = 30\%$ and the two fixed values of nonlocal parameters ($\xi = 0$ and $\xi = 0.5$), the distributions of physical field variables such as temperature, moisture, mechanical, and plasma are shown in Figure 4A–D. At $\xi = 0.5$, the basic physical wave distributions have been well-defined. In virtually all cases, the absolute value of these field variables is close to zero. At this value of the non-local parameter, the bending of these field variables becomes quite large. To be more specific, the nonlocality parameter has a profound impact on the primary physical distributions.

8 Conclusion

In this study, we investigate how several external conditions, such as ramp-type heating, laser shock, moisture, and mechanical forces, might affect the propagation of photothermal-elastic waves in a solid non-local semiconducting medium. Electron-elastic deformations ignite elastic waves inside the non-local semiconductor, resulting in a fluctuating deformation potential. One may get the 1D case now. There is hope that the photo-thermoelasticity theories may focus attention on the peculiarities of wave motion in non-local semiconductor media. Considerable graphical analysis has been performed to investigate the significance of thermal memory, the variable thermal conductivity effect, nonlocality, and the moisture reference. As a result of its clarity and precision, the photothermal theory may be used to explain de-excitation in materials and the absorption of light. The plots show that the thermal memory, thermal conductivity, moisture content, and nonlocality of the medium have a major impact on all the considered domains. The research might help scientists learn more about how waves behave in a wide range of environments and temperatures. There is a clear correlation between the thermal conductivity, moisture content, and nonlocality of the field quantities, as the amplitude of these values varies (increasing or decreasing) with the thermal memory. Recent research has shown that semiconductors may be utilized to convert solar energy into electricity while also withstanding exposure to laser pulses, demonstrating the vital role that semiconductors play in today's cutting-edge technologies. Modern technology relies heavily on semiconductors in a variety of devices, such as solar cells, displays, and transistors. Several fields of mechanical and electrical engineering employ them as nanomaterials. Thermomechanical, sensor, resonator, medical, and accelerometer researchers should all be able to make use of the study's findings in their own ongoing and future investigations. At the opposite end of the spectrum, microwave and radio frequency emitters make it possible for people to communicate wirelessly. Visible and infrared diode lasers are at the center of the information technology industry. The method presented here has potential application to a wide range of photo-thermoelasticity and thermodynamic issues.

Data availability statement

The original contributions presented in the study are included in the article/Supplementary Material, further inquiries can be directed to the corresponding authors.

Author contributions

KL: Supervision, conceptualization, methodology, software, data curation. SE-S: Writing—original draft preparation. HC: Visualization, investigation. AE-B: Software, validation, NB: New Software; writing—reviewing and editing.

Acknowledgments

Authors extend their appreciation to Princess Nourah bint Abdulrahman University for fund this research under Researchers Supporting Project number (PNURSP2023R154) Princess Nourah bint Abdulrahman University, Riyadh, Saudi Arabia.

The authors extend their appreciation to the Deanship of Scientific Research at Northern Border University, Arar, KSA for funding this research work through the project number "NBU-FFR-2023-0027".

Conflict of interest

The authors declare that the research was conducted in the absence of any commercial or financial relationships that could be construed as a potential conflict of interest.

Publisher's note

References

Abo-dahab, S., and Lotfy, Kh. (2017). Two-temperature plane strain problem in a semiconducting medium under photothermal theory. *Waves Ran. Comp. Med.* 27 (1), 67–91. doi:10.1080/17455030.2016.1203080

Abouelregal, A., and Marin, M. (2020). The response of nanobeams with temperature-dependent properties using state-space method via modified couple stress theory. *Symmetry* 12 (8), 1276. doi:10.3390/sym12081276

Alhashash, A., Elidy, E., El-Bary, A., Tantawi, R., and Lotfy, Kh. (2022). Two-temperature semiconductor model photomechanical and thermal wave responses with moisture diffusivity process. *Crystals* 12, 1770. doi:10.3390/cryst12121770

Allen, P. B. (2014). Size effects in thermal conduction by phonons. *Phys. Rev. B* 90, 054301. doi:10.1103/physrevb.90.054301

Biot, M. A. (1956). Thermoelasticity and irreversible thermodynamics. *J. Appl. Phys.* 27, 240–253. doi:10.1063/1.1722351

Brancik, L. "Programs for fast numerical inversion of Laplace transforms in MATLAB language environment," in Proceedings of the 7th Conf. MATLAB'99, Czech Republic Prague, November 1999, 27–39.

Chandrasekharaiah, D. S. (1986). Thermoelasticity with second sound: A review. *Appl.Mech. Rev.* 39, 355–376. doi:10.1115/1.3143705

Eringen, A., and Edelen, D. (1972). On nonlocal elasticity. *Int. J. Eng. Sci.* 10, 233–248. doi:10.1016/0020-7225(72)90039-0

Eringen, A. (1972). Nonlocal polar elastic continua. *Int. J. Eng. Sci.* 10, 1–16. doi:10.1016/0020-7225(72)90070-5

Ezzat, M. (2020). Hyperbolic thermal-plasma wave propagation in semiconductor of organic material. *Waves Rand. Comp. media* 32, 334–358. doi:10.1080/17455030.2020.1772524

Gasch, A., Malm, R., and Ansell, A., 2016, Coupled hygro-thermomechanical model for concrete subjected to variable environmental conditions, *Int. J. Solids Struct.*, 91, 143–156.

Gordon, J. P., Leite, R. C. C., Moore, R. S., Porto, S. P. S., and Whinnery, J. R. (1964). Long-transient effects in lasers with inserted liquid samples. *Bull. Am. Phys. Soc.* 119, 501.

Green, A. E., and Lindsay, K. A. (1972). Thermoelasticity. *J. Elast.* 2, 1–7. doi:10.1007/bf00045689

Hasselman, D., and Heller, R. (1980). *Thermal stresses in severe environments*. New York, USA: Plenum Press.

Hasselman, D., and Heller, R. (1980). *Thermal stresses in severe environments*. New York, NY, USA: Plenum Press.

Hobiny, A., and Abbas, I. A. (2016). A study on photothermal waves in an unbounded semiconductor medium with cylindrical cavity. *Mech. Time-Depend Mater* 6, 61–72. doi:10.1007/s11043-016-9318-8

Honig, G., and Hirdes, U. (1984). A method for the numerical inversion of Laplace transforms Transforms. *Comp. Appl. Math.* 10 (1), 113–132. doi:10.1016/0377-0427(84)90075-x

Hosseini, S. M., Sladek, J., and Sladek, V. (2013). Application of meshless local integral equations to two dimensional analysis of coupled non-Fick diffusion-elasticity. *Eng. Analysis Bound. Elem.* 37 (3), 603–615. doi:10.1016/j.enganabound.2013.01.010

Huang, M., Wei, P., Zhao, L., and Li, Y. (2021). Multiple fields coupled elastic flexural waves in the thermoelastic semiconductor microbeam with consideration of small scale effects. *Compos. Struct.* 270, 114104. doi:10.1016/j.compstruct.2021.114104

Khamis, A., Lotfy, Kh., El-Bary, A., Mahdy, A., and Ahmed, M. (2021). Thermal-piezoelectric problem of a semiconductor medium during photo-thermal excitation. *Waves Random Complex Media* 31 (6), 2499–2513. doi:10.1080/17455030.2020.1757784

Kreuzer, L. B. (1971). Ultralow gas concentration infrared absorption spectroscopy. *J. Appl. Phys.* 42, 2934–2943. doi:10.1063/1.1660651

Liu, J., Han, M., Wang, R., Xu, S., and Wang, X. (2022). Photothermal phenomenon: Extended ideas for thermophysical properties characterization. *J. Appl. Phys.* 131, 065107. doi:10.1063/5.0082014

Lord, H., and Shulman, Y. (1967). A generalized dynamical theory of thermoelasticity. *J. Mech. Phys. Solids* 15, 299–309. doi:10.1016/0022-5096(67)90024-5

Lotfy, Kh., Hassan, W., and Gabr, M. E. (2017). Thermomagnetic effect with two temperature theory for photothermal process under hydrostatic initial stress. *Results Phys.* 7, 3918–3927. doi:10.1016/j.rinp.2017.10.009

Lotfy, Kh. (2017). Photothermal waves for two temperature with a semiconducting medium under using a dual-phase-lag model and hydrostatic initial stress. *Waves Ran. Comp. Med.* 27 (3), 482–501. doi:10.1080/17455030.2016.1267416

Lotfy, Kh., and Tantawi, R. (2020). Photo-thermal-elastic interaction in a functionally graded material (FGM) and magnetic field. *Silicon* 12, 295–303. doi:10.1007/s12633-019-00125-5

Lotfy, Kh. (2016). The elastic wave motions for a photothermal medium of a dual-phase-lag model with an internal heat source and gravitational field. *Can. J. Phys.* 94, 400–409. doi:10.1139/cjp-2015-0782

Marin, M., Ellahi, R., Vlase, S., and Bhatti, M. (2020). On the decay of exponential type for the solutions in a dipolar elastic body. *J. Taibah Univ. Sci.* 14 (1), 534–540. doi:10.1080/16583655.2020.1751963

Marin, M., Vlase, S., and Paun, M. (2015). Considerations on double porosity structure for micropolar bodies. *AIP Adv.* 5 (3), 037113. doi:10.1063/1.4914912

Mondal, S., and Sur, A. (2021). Photo-thermo-elastic wave propagation in an orthotropic semiconductor with a spherical cavity and memory responses. *Waves Random Complex Media* 31 (6), 1835–1858. doi:10.1080/17455030.2019.1705426

Scutaru, M., Vlase, S., Marin, M., and Modrea, A. New analytical method based on dynamic response of planar mechanical elastic systems, *Bound. Value Probl.*, 2020, 1, 104, doi:10.1186/s13661-020-01401-9

Sladek, J., Sladek, V., Repka, M., and Pan, E. (2020). A novel gradient theory for thermoelectric material structures. *Int. J. Solids Struct.* 206, 292–303. doi:10.1016/j.ijsolstr.2020.09.023

Song, Y. Q., Todorovic, D. M., Cretin, B., and Vairac, P. (2010). Study on the generalized thermoelastic vibration of the optically excited semiconducting microcantilevers. *Int. J. Sol. Struct.* 47, 1871–1875. doi:10.1016/j.ijsolstr.2010.03.020

Szekeres, A. (2000). Analogy between heat and moisture. *Comput. Struct.* 76, 145–152. doi:10.1016/s0045-7949(99)00170-4

Szekeres, A., 2012, Cross-coupled heat and moisture transport: Part 1 theory, *J. Therm. Stresses*, 35, 248–268.

Szekeres, A., and Engelbrecht, J., 2000, Coupling of generalized heat and moisture transfer, *Period. Polytech. Ser. Mech. Eng.*, 44, (1), 161–170.

Tam, A. C. (1986). Applications of photoacoustic sensing techniques. *Rev. Mod. Phys.* 58, 381–431. doi:10.1103/revmodphys.58.381

Tam, A. C. (1989). *Photothermal investigations in solids and fluids*. Boston, Unites States: Academic Press, 1–33.

Tam, A. C. (1983). *Ultrasensitive laser spectroscopy*. New York, NY, USA: Academic Press, 1–108.

Todorovic, D. M., Nikolic, P. M., and Bojicic, A. I. (1999). Photoacoustic frequency transmission technique: Electronic deformation mechanism in semiconductors. *J. Appl. Phys.* 85, 7716–7726. doi:10.1063/1.370576

Vlase, S., Năstac, C., Marin, M., and Mihălcică, M. (2017). A method for the study of the vibration of mechanical bars systems with symmetries. *Acta Tech. Napoc. Ser. Appl. Math. Mech. Eng.* 60 (4), 539–544.

Youssef, H., and Abbas, I. (2007). Thermal shock problem of generalized thermoelasticity for an infinitely long annular cylinder with variable thermal conductivity. *Comp. Meth. Sci. Tech.* 13, 95–100. doi:10.12921/cmst.2007.13.02.95-100

Youssef, H., and Abbas, I. (2007). Thermal shock problem of generalizedthermoelasticity for an infinitely long annular cylinder with variable thermal conductivity. *Comput. methods Sci. Technol.* 13 (2), 95–100. doi:10.12921/cmst.2007.13.02.95-100

Youssef, H., and El-Bary, A. (2006). Thermal shock problem of a generalized thermoelastic layered composite material with variable thermal conductivity. *Math. Problems Eng.* 2006, 1–14. doi:10.1155/mpe/2006/87940

Youssef, H. (2005). State-space on generalized thermoelasticity for an infinite material with a spherical cavity and variable thermal conductivity subjected to ramp-type heating. *J. CAMQ, Appl. Math. Inst.* 13, 369–390.

Zhao, L., Wei, P., Huang, M., and Xu, Y. (2022). Electro-Thermo-Mechanical multiple fields coupled wave propagation through piezoelectric semiconductor sandwich structure. *Compos. Struct.* 288, 115358. doi:10.1016/j.compstruct.2022.115358

Zhao, L., Wei, P., Huang, M., and Xu, Y. (2022). Reflection and transmission of coupled elastic waves by a semiconduction interlayer with consideration of photothermal effects. *J. Acoust. Soc. Am.* 151 (3), 1816–1828. doi:10.1121/10.0009674

10.3389/fmats.2023.1193423

Nomenclature

$\boldsymbol{\lambda, \mu}$	Lame's elastic parameters
$\boldsymbol{\delta_n = (3\lambda + 2\mu)d_n}$	The deformation potential difference
$\boldsymbol{T_0}$	Reference temperature in its natural state
$\boldsymbol{\gamma_t = (3\lambda + 2\mu)\alpha_T}$	The volume thermal expansion
$\boldsymbol{N_0}$	The equilibrium carrier concentration
$\boldsymbol{\rho}$	The density of the non-local medium
$\boldsymbol{\alpha_T}$	Coefficients of linear thermal expansion
$\boldsymbol{C_e}$	Specific heat of the microelongated material at constant strain
$\boldsymbol{D_E}$	The carrier diffusion coefficient
$\boldsymbol{\tau}$	The carrier lifetime
$\boldsymbol{E_g}$	The energy gap
$\boldsymbol{d_n}$	The coefficients of electronic deformation
$\boldsymbol{\beta_{ij}, \beta_{ij}^m}$	The isothermal and elastic coupling coefficients of moisture
$\boldsymbol{\varepsilon_{kl}}$	The strain tensor
$\boldsymbol{C_{ijkl}}$	The isothermal parameters tensor
$\boldsymbol{\tau_0, v_0}$	Thermal relaxation times
$\boldsymbol{D_T}$	The temperature diffusivity
$\boldsymbol{D_m}$	The diffusion coefficient of moisture
$\boldsymbol{\sigma_{ij}}$	The stress tensor
$\boldsymbol{\delta_{ik}}$	Kronecker delta
$\boldsymbol{D_T^m, D_m^T}$	The coupled diffusivities
$\boldsymbol{m_0}$	The reference moisture
$\boldsymbol{K_m}$	The moisture thermal conductivity
$\frac{1}{k} = \frac{\rho C_E}{K_0}$	The thermal diffusivity